Molecular Therapy
Methods & Clinical Development
Original Article

Thermal Stability as a Determinant of AAV Serotype Identity

Antonette Bennett,[1] Saajan Patel,[1] Mario Mietzsch,[1] Ariana Jose,[1] Bridget Lins-Austin,[1,3] Jennifer C. Yu,[1] Brian Bothner,[2] Robert McKenna,[1] and Mavis Agbandje-McKenna[1]

[1]Department of Biochemistry and Molecular Biology, Center for Structural Biology, The McKnight Brain Institute, College of Medicine, University of Florida, Gainesville, FL 32610, USA; [2]Department of Chemistry and Biochemistry, Montana State University, Bozeman, MT 59715, USA

Currently, there are over 150 ongoing clinical trials utilizing adeno-associated viruses (AAVs) to target various genetic diseases, including hemophilia (AAV2 and AAV8), congenital heart failure (AAV1 and AAV6), cystic fibrosis (AAV2), rheumatoid arthritis (AAV2), and Batten disease (AAVrh.10). Prior to patient administration, AAV vectors must have their serotype, concentration, purity, and stability confirmed. Here, we report the application of differential scanning fluorimetry (DSF) as a good manufacturing practice (GMP) capable of determining the melting temperature (T_m) for AAV serotype identification. This is a simple, rapid, cost effective, and robust method utilizing small amounts of purified AAV capsids (~25 μL of ~10^{11} particles). AAV1-9 and AAVrh.10 exhibit specific T_ms in buffer formulations commonly used in clinical trials. Notably, AAV2 and AAV3, which are the least stable, have varied T_ms, whereas AAV5, the most stable, has a narrow T_m range in the different buffers, respectively. Vector stability was dictated by VP3 only, specifically, the ratio of basic/acidic amino acids, and was independent of VP1 and VP2 content or the genome packaged. Furthermore, stability of recombinant AAVs differing by a single basic or acidic amino acid residue are distinguishable. Hence, AAV DSF profiles can serve as a robust method for serotype identification of clinical vectors.

INTRODUCTION

Adeno-associated viruses (AAVs) are small, ~260 Å, T = 1, icosahedral non-enveloped viruses belonging to the *Dependoparvovirus* genus of the *Parvoviridae* family. Their capsids serve as vehicles to deliver viral-packaged genomes to the nucleus for replication. Currently, 13 human and non-human primate AAV serotypes and over 150 genotypes have been identified.[1] The AAV capsid is composed of 60 copies in total of viral protein (VP)1 (~87 kDa), VP2 (~73 kDa), and VP3 (~61 kDa) in a population ratio of 1:1:10, respectively.[2,3] The AAV VPs share a common VP3 C-terminal sequence, with VP1 and VP2 extended at their N-termini. The VP1 is further N-terminally extended compared to VP2, with the VP1 unique (VP1u) region containing a phospholipase A2 (PLA2) domain, required for infectivity.[4,5] Differences in amino acid sequence and capsid structure mediate the interaction of the AAV serotypes with different host cell receptors, leading to alternative cell or tissue tropisms. For example, AAV1 has tropism for skeletal muscle, whereas AAV8 has tropism for the liver (reviewed by Hastie et al.[6]).

AAV gene therapy has developed into one of the lead treatment strategies for various monogenetic diseases. These vectors are recombinant AAVs (rAAVs), with a transgene expression cassette packaged instead of the wild-type (WT) viral genome.[7] Early development of the AAV gene therapy system was mostly focused on AAV2.[8] However, novel AAV serotypes have been isolated, along with the discovery that some of these viruses exhibit higher transduction efficiencies in certain cells or tissues compared to AAV2. This led to a larger repertoire of available capsids for packaging different therapeutic genes.[9,10] Thus, many recent clinical trials have utilized a range of AAV serotypes for therapeutic gene delivery.[11–13] Significantly, a rAAV1 vector for treating lipoprotein lipase deficiency is the first approved human gene therapy biologic and was certified by the European Medical Agency.[12]

The AAVs share high amino acid sequence identity, resulting in a need to develop methods for confirming the serotype in clinical grade vectors prior to administration. However, in contrast to WT AAV packaging unique genomes, the identity of purified rAAV capsids cannot be determined by PCR-based sequencing methods. Furthermore, although mouse monoclonal antibodies are available for some of the AAV serotypes, which can identify their capsids, this is not the case for all available AAVs.[14–17] The engineering of AAVs for various reasons, including escape from pre-existing neutralizing host antibodies or improved tissue targeting, which modifies antigenic regions, compounds this problem. An alternative for capsid identification of purified rAAV preparation is mass spectrometry.[18] This method has several advantages, including small sample size (~0.5–5 μg), a low percentage of unique peptide coverage for identification, and single residue variations that can be detected when

Received 12 March 2017; accepted 18 July 2017;
http://dx.doi.org/10.1016/j.omtm.2017.07.003.

[3]Present address: Division of Viral Products, CBER/FDA, Silver Spring, MD 20993, USA

Correspondence: Mavis Agbandje-McKenna, Department of Biochemistry and Molecular Biology, Center for Structural Biology, The McKnight Brain Institute, College of Medicine, University of Florida, Gainesville, FL 32610, USA.
E-mail: mckenna@ufl.edu

This is an open access article under the CC BY-NC-ND license (http://creativecommons.org/licenses/by-nc-nd/4.0/).

compared to the WT AAV sequence. However, disadvantages include the requirement for serotype-specific proteases, manual manipulation of the sample, and time required to prepare and analyze the sample. This includes running a denatured gel, peptide digest, mass analysis, and database search.[18] Thus, there is a need for new or improved methods for rAAV serotype identification.

Here, we report the application of differential scanning fluorimetry (DSF), capable of accurate melting temperature (T_m) determination, for AAV serotype identification. This approach was developed and applied to the characterization of AAV capsid stability as previously described.[35] This is a simple, cost effective, rapid, and robust method utilizing small amounts of purified rAAV capsids ($\sim 10^{11}$ particles) and a dye (SYPRO Orange). This study analyzed AAV1–AAV9 and AAVrh.10, where AAV3 refers specifically to AAV3b. The AAV serotypes displayed specific capsid stabilities in buffers commonly used for their formulation and storage, with a single amino acid difference being detectable. The T_m is dictated by the VP3 sequence alone, and not VP1, VP2, or the packaged genome, making it an ideal method for clinical sample authentication.

RESULTS

Stability of rAAV1–rAAV9 and rAAVrh.10 in PBS Buffer Shows Disparate Profiles

The stability of rAAV1–rAAV9 and rAAVrh.10 in PBS, the most commonly utilized AAV formulation and storage buffer, was analyzed using DSF. The AAV samples were produced using the Baculovirus/*Spodoptera Frugiperda* 9 (*Sf*9) cell expression system or in HEK293 cells, and purified by AVB affinity column chromatography, with genome-containing (full) and empty capsids separated by sucrose sedimentation gradient, as previously described.[19–21] Sample purity and capsid integrity were confirmed by SDS-PAGE and negative-stain electron microscopy (EM), respectively (Figure 1A). The T_m for the purified full and empty capsids, diluted into PBS buffer, was determined by DSF,[22] as described in Materials and Methods. The T_m is the temperature at which 50% of the sample is unfolded and bound with dye. The thermal profiles show T_ms ranging from 66.5°C to 89.5°C ± 0.5°C, with rAAV2 being the least stable and rAAV5 being the most stable, respectively (Figure 1B; Table 1). The T_m of each AAV was unique, with the exception of AAV7, rAAV9, and rAAVrh.10 at 77.0°C ± 0.1°C–0.8°C, which could not be distinguished within experimental error (Figure 1B; Table 1). Significantly, the full and empty capsid T_ms were similar for all the AAVs tested (Table 1).

Comparative Stability Analysis of rAAV1–rAAV9 and rAAVrh.10 in Commonly Used Formulation and Storage Buffers Reveals Serotype-Specific Stabilities

The observation that rAAV9 and rAAVrh.10 exhibited experimentally the same T_m in PBS buffer, and the knowledge that the composition, ionic strength, and pH of a buffer could have an impact on T_m led to further investigation of thermal stability profiles in other commonly used AAV formulation and storage buffers (Table 1). The stability of purified full and empty capsids for rAAV1–AAV9 and rAAVrh.10, diluted 10x into five additional (to PBS) common buffers and universal buffer (UB), developed to be insensitive to pH changes during thermal melting experiments,[23] was tested. The T_ms for each AAV in the buffers aligned into three groups: group I was AAVs with T_ms varying by ~15°C–20°C, AAV2 and AAV3; group II was AAVs with T_ms varying by ~3°C–6°C, AAV1, AAV4, AAV6, AAV7, AAV8, and AAVrh.10; and group III was AAVs with T_ms varying by <2.0°C, AAV5 and AAV9 (Figures 2A–2J; Table 1). Comparative analysis of the AAVs in the different buffers showed that each buffer had a different effect on each serotype, i.e., no buffer caused a consistent stabilization or destabilization of all ten viruses tested (Figure 2K; Table 1). Of note, only minor T_m fluctuations, ~1°C–2°C, were observed between full and empty capsids of a few AAVs, whereas most showed no detectable T_m difference (Figure 3; Table 1). For T_ms showing minor differences, there was no trend of full or empty capsids being more or less stable.

Small Volume and Low Concentration Requirement of AAV Samples for DSF Analysis

An important aspect of developing DSF profiling as a method for determining capsid stability and serotype identity was to determine the minimal amount of AAV required for the assay. Thus, purified full and empty capsids of AAV5, the most stable serotype, were tested at starting concentrations of 5×10^{13} viral genome (vg)/mL and 3.4×10^{13} particles/mL, respectively. The samples serially diluted 10–100x into PBS and followed by T_ms determination identified a minimal concentration at which signal could be measured. The lowest detectable concentrations for the full and empty capsids were 5×10^{11} vg/mL and 3.4×10^{11} particles/mL, respectively, tested in 25 µL (Figures 4A and 4B).

AAV VP3 Is the Determinant of Capsid Stability

Following the observation that the genome had only a minor effect on the AAV stability, the role of VP1, VP2, and VP3 on capsid stability was analyzed for AAV2, the serotype exhibiting the lowest capsid stability (Figure 1B; Table 1). AAV2 virus-like particles (VLPs) assembled from (1) VP1, VP2, and VP3 (AAV2-VP123); (2) VP1 and VP3 only (AAV2-VP13), (3) VP2 and VP3 only (AAV2-VP23), and (4) VP3 only (AAV2-VP3) were generated by the site-directed mutagenesis of the start codon of the respective VP to be eliminated in the pFBDVPm11 plasmid.[24] The VLPs were produced and purified, as described in Materials and Methods, and diluted into PBS for T_m analysis by DSF. SDS-PAGE (silver stained) and negative-stain EM showed the correct VP content for each construct and intact capsid assembly (Figure 5A). The T_ms for the WT VLPs and VP variant VLPs were superposable and their mean T_m was ~67.5°C ± 0.5°C (Figure 5B). In this assay, AAV5 VLPs were included as a control sample and its T_m was measured at 90°C ± 0.5°C, which is within experimental error of the value obtained from the samples produced in the *OneBac* system[19] and used for the assays reported above (Figure 5B). These data showed that VP3 is sufficient to assemble the virus capsid, as previously reported,[25–27] and that its sequence is the sole determinant of the capsid stability.

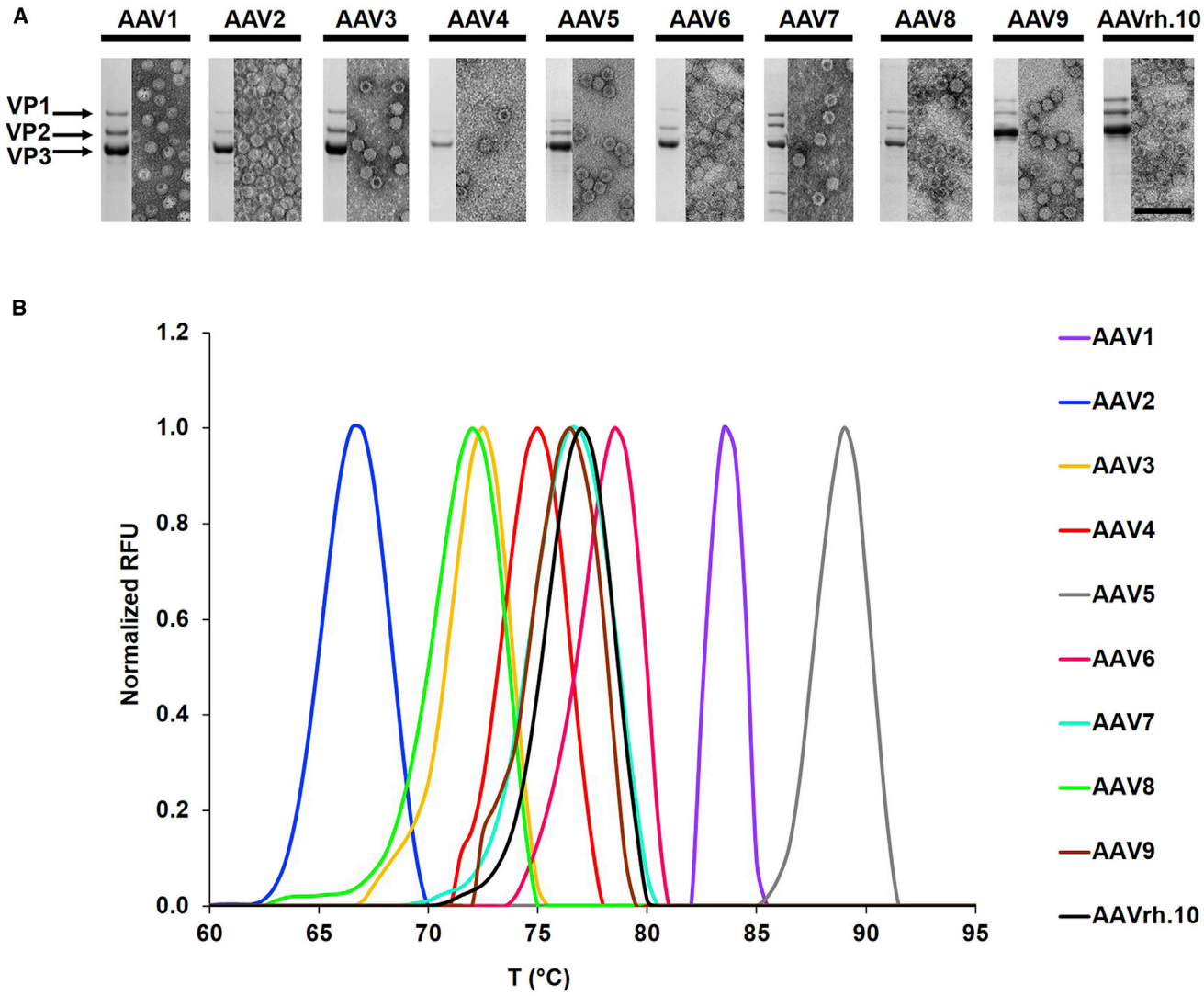

Figure 1. Sample Evaluation and Stability of Full rAAV1–rAAV9-gfp and rAAVrh.10-gfp, Packaging the GFP Transgene, Vectors in PBS

(A) Coomassie blue stained SDS-PAGE (left) and negative-stained EM (right) of rAAV1–rAAV9 and rAAVrh.10 as indicated above each panel. Scale bar, 100 nm, is shown in the AAVrh.10 EM image. (B) Thermal profile (shown as normalized relative fluorescence units [RFUs]) versus temperature (T [°C]) of rAAV1–rAAV9 and rAAVrh.10 obtained by DSF analysis. A representative profile is shown for each serotype. See also Table 1. Each profile is colored according to the serotype, as shown on the right-hand side.

The observation that VP3 was the determinant of AAV capsid stability initiated a comparative analysis of the sequences of the AAVs. The sequence identity between the ten AAVs was calculated using the Clustal Omega application[28] (data not shown), and calculation of the isoelectric point (pI) and analysis of the number of basic and acidic residues were conducted using the ExPASy application.[29] The sequence identity between the AAVs range from ~55%, between AAV4 and AAV5 and between them and the other AAVs, to 99% between AAV1 and AAV6 (data not shown), consistent with previous reports.[1,18] A reversed relationship was observed between the T_m of each AAV in PBS and UB when plotted with the calculated pI, with the exceptions being AAV4 and AAV6 (Figure 6). These viruses both had a higher pI than was expected in the overall trend, in which AAV5, with the lowest calculated pI, was the most stable serotype. The data indicated a potential role of the acidic and basic residues (reflected in the pI) in dictating the stability of the AAV capsid.

T_m Distinguishes a Single Acidic or Basic Amino Acid Residue Difference in an AAV Variant

The validity of the prediction that VP3 sequence and pI, particularly the ratio of basic to acidic resides, is a determinant of AAV stability, was tested by comparing AAV1 and AAV6, which differ by six amino acids, including one acidic/basic amino acid, E531K. Reciprocal variants, AAV1-E531K and AAV6-K531E[30] and AAV1 and AAV6 packing the luciferase gene were analyzed by DSF. The T_ms for AAV1, AAV1-K531, AAV6, and AAV6-E531 were 84.0°C,

Table 1. T_m of AAV1–AAV9 and AAVrh.10 Full and Empty Capsids in Different Buffers

Buffer	AAV1 Full	AAV1 Empty	AAV2 Full	AAV2 Empty	AAV3 Full	AAV3 Empty	AAV4 Full	AAV4 Empty	AAV5 Full	AAV5 Empty
PBS	83.5 ± 0.1	83.8 ± 0.3	68.2 ± 0.6	67.3 ± 0.8	71.7 ± 1.0	71.2 ± 1.2	75.0 ± 0.7	75.0 ± 0.5	89.2 ± 0.1	89.2 ± 0.3
CiPO4	83.0 ± 0.1	83.2 ± 0.6	67.2 ± 0.6	65.5 ± 0.9	67.8 ± 0.8	68.2 ± 0.3	73.3 ± 1.1	74.0 ± 0.5	89.2 ± 0.1	89.2 ± 0.3
HEPES	85.0 ± 0.1	85.0 ± 0.9	76.8 ± 0.3	77.5 ± 0.5	82.7 ± 0.6	83.0 ± 0.1	77.0 ± 0.7	76.0 ± 0.5	88.7 ± 0.1	88.7 ± 0.3
Tris	86.0 ± 0.1	85.0 ± 2.2	79.7 ± 0.3	80.2 ± 0.3	86.8 ± 0.3	86.8 ± 0.1	76.5 ± 2.1	77.5 ± 0.5	88.7 ± 0.3	88.7 ± 0.3
LR	84.5 ± 0.9	84.7 ± 0.6	75.2 ± 0.3	76.0 ± 1.8	78.5 ± 4.0	79.0 ± 2.5	75.3 ± 0.4	75.5 ± 0.5	89.0 ± 0.1	89.0 ± 0.1
BSS	84.3 ± 0.3	84.2 ± 0.3	71.2 ± 0.6	70.7 ± 1.8	76.3 ± 1.2	76.8 ± 0.3	75.5 ± 0.7	76.0 ± 0.5	89.3 ± 0.1	89.3 ± 0.3
UB	85.3 ± 0.3	85.0 ± 0.5	76.3 ± 0.3	75.0 ± 1.3	81.0 ± 0.9	82.5 ± 2.8	77.8 ± 0.4	77.5 ± 0.5	89.0 ± 0.1	89.0 ± 0.1
Buffer	AAV6 Full	AAV6 Empty	AAV7 Full	AAV7 Empty	AAV8 Full	AAV8 Empty	AAV9 Full	AAV9 Empty	AAV10 Full	AAV10 Empty
PBS	77.5 ± 0.6	78.5 ± 0.9	76.5 ± 0.1	76.7 ± 0.3	72.0 ± 0.1	71.2 ± 0.6	77.0 ± 0.3	77.0 ± 0.5	77.0 ± 0.8	77.0 ± 0.1
CiPO4	78.8 ± 1.3	79.3 ± 0.3	75.2 ± 0.3	75.0 ± 0.1	71.0 ± 0.3	71.2 ± 0.6	76.7 ± 0.3	76.5 ± 0.1	76.5 ± 0.1	76.0 ± 0.1
HEPES	81.3 ± 0.9	81.3 ± 0.5	76.5 ± 0.1	76.0 ± 0.1	72.0 ± 0.3	71.2 ± 0.6	77.3 ± 1.0	77.5 ± 0.3	77.5 ± 0.3	77.3 ± 0.3
Tris	80.7 ± 0.6	81.8 ± 1.2	78.0 ± 0.1	78.5 ± 0.1	73.5 ± 0.3	72.0 ± 0.9	78.2 ± 0.5	78.2 ± 0.3	78.2 ± 0.3	79.7 ± 0.6
LR	79.7 ± 2.2	80.2 ± 1.5	78.0 ± 0.1	78.0 ± 0.1	73.9 ± 1.0	72.7 ± 1.2	77.5 ± 0.3	78.3 ± 0.5	78.3 ± 0.5	78.3 ± 0.6
BSS	79.5 ± 0.5	79.5 ± 0.3	78.0 ± 0.1	77.3 ± 0.3	73.1 ± 0.3	72.5 ± 0.9	77.2 ± 0.5	78.0 ± 0.3	78.0 ± 0.3	78.8 ± 1.4
UB	80.8 ± 1.5	80.8 ± 3.0	78.5 ± 0.1	77.2 ± 0.3	73.3 ± 0.8	73.0 ± 0.1	77.5 ± 0.3	78.5 ± 0.9	78.5 ± 0.9	78.5 ± 0.6

Buffer abbreviations and formulations are provided in the Materials and Methods.

78.0°C, 79.0°C, and 83.5°C, respectively. The T_m for AAV1-K531 was similar to that of AAV6, whereas that of AAV6-E531 was similar to that of AAV1 (Figure 5C). Thus, mutation of AAV1 residue E531 to K resulted in destabilization, whereas mutation of AAV6 K531 to E resulted in stabilization (Figure 5C).

Capsid Stability in Different Buffer Formulations Shows No Significant Effect on AAV Transduction Efficiency

To determine if the difference in stability observed in different buffer formulations translated to transduction efficiency, luciferase gene expression by four AAV serotypes belonging to group I (AAV2), II (AAV1 and AAV8), and III (AAV5), diluted into the different buffers, was tested in HEK293 cells. These four serotypes were selected not only to represent the stability groups defined for the AAVs, but also because they represent the range of sequence identity and structural diversity between the AAV serotypes. AAV2 transduces HEK293 more efficiently than AAV1 (23% of AAV2), AAV5 (2% of AAV2), and AAV8 (2% of AAV2) based on mean relative light unit (RLU). Comparison of the transduction efficiency (TE) of all four vectors, normalized to the PBS data, did not differ significantly for each serotype in the respective buffers (Figure 7). Similarly, there was no correlation between the T_m and TE of each AAV in the different buffers, except for AAV8, which displayed a minor upward trend (Figure 7). This observation is consistent with the cell culture media, into which the viruses, previously exposed to different buffers, are diluted by 10X, serving as the determinant of the virus properties and not the formulation buffers. This observation was anticipated because dilution of the viruses from Tris-HCl, utilized for neutralization after purification, into the different formulation buffers dictated their thermostability, as presented above. Thus, when working at a physiological or close to physiological pH, AAV vector storage buffer formulations dictate stability. However, the extracellular environment would dictate rAAV vector performance in vitro and likely in vivo.

DISCUSSION

The use of AAVs as a clinical gene therapy vector requires good manufacturing practice (GMP), with the characterization of the final product to include certification of purity, stability, genome titer, infectious titer, and absence of endotoxins, according to Food and Drug Administration (FDA) requirements (reviewed by Wright[31]). In this study, we developed a DSF protocol that determines the thermal profile or T_m of AAV capsids as a method for serotype identification. The reported dosage of AAVs utilized in several clinical and preclinical trials is 10^{12}–10^{13} vg/kg or 10^{11}–10^{14} vg/patient.[32–34] The application of DSF for serotype identification required minimal samples of ~10^{11} vg/mL or particles/mL for full and empty capsids, respectively, in 22.5 µL of total volume to obtain a measurable fluorescence enabling T_m calculation (Figures 4A and 4B). This amount of material is easily attainable in therapeutic samples, making DSF a suitable approach for the proposed serotype identification.

Significantly, the distinct T_m of each AAV serotype in different buffer formulations enables their identification in ~1 hr. The T_m of AAV1–AAV9 and AAVrh.10 was a unique identifier for each serotype, with the exception of AAV7, AAV9, and AAVrh.10 in PBS, which were similar (Figure 1B; Table 1). These serotypes could, however, be distinguished based on their T_m measured in other buffers (Figure 2; Table 1). For example, AAV9 showed almost no variation in T_m in a different buffer formulation, whereas AAV7 showed a 3°C variation of T_m in the same buffers (Figures 2G and 2I), providing additional means for distinguishing the two viruses. A previous comparative

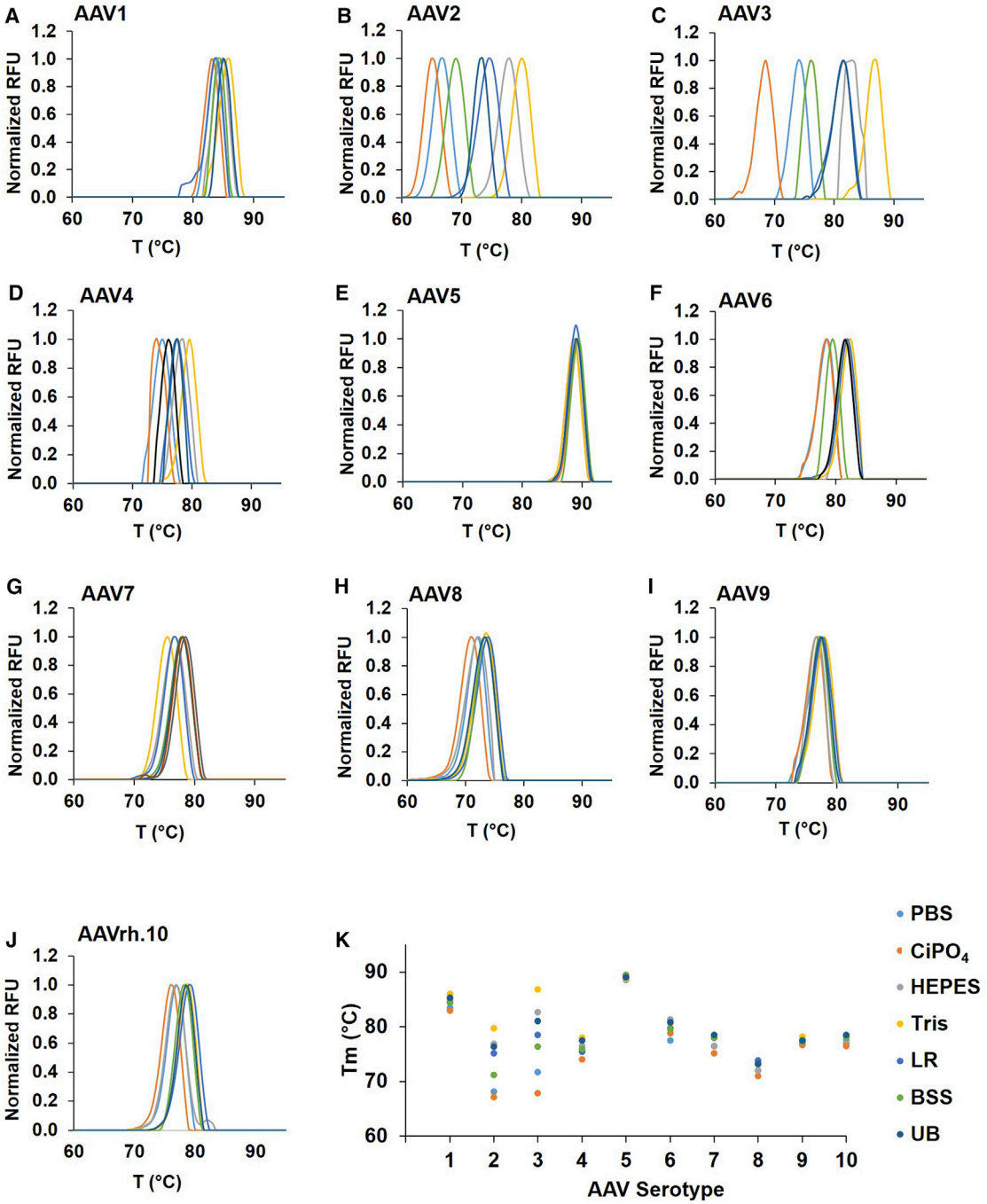

Figure 2. Comparative Thermal Profiles of Full AAV1–AAV9-gfp and AAVrh.10-gfp Capsids in Commonly Used AAV Formulation and Storage Buffers and UB

(A–J) Comparison of (A) AAV1, (B) AAV2, (C) AAV3, (D) AAV4, (E) AAV5, (F) AAV6, (G) AAV7, (H) AAV8, (I) AAV9, and (J) AAVrh.10 thermal profiles (shown as in Figure 1) in different buffers. Each buffer profile is colored according to the series legend in (K). (K) Discrete dots representing the distribution of T_ms (°C) for each AAV serotype in the different buffers, as indicated to the right-hand side.

analysis of AAV capsid stability and capsid dynamics for AAV1, AAV2, AAV5, and AAV8 introduced DSF as a method for distinguishing AAV serotypes based on stability.[35] The T_m obtained for AAV1, AAV2, AAV5, and AAV8 in this previous study[35] in the PBS buffer used is consistent with our observations. In other studies of AAV2 and AAV5 in the lactate ringer (LR) and balanced salt solution (BSS) buffers, similar T_ms to those obtained in our study were reported.[36,37] More recently, another group utilized this DSF approach

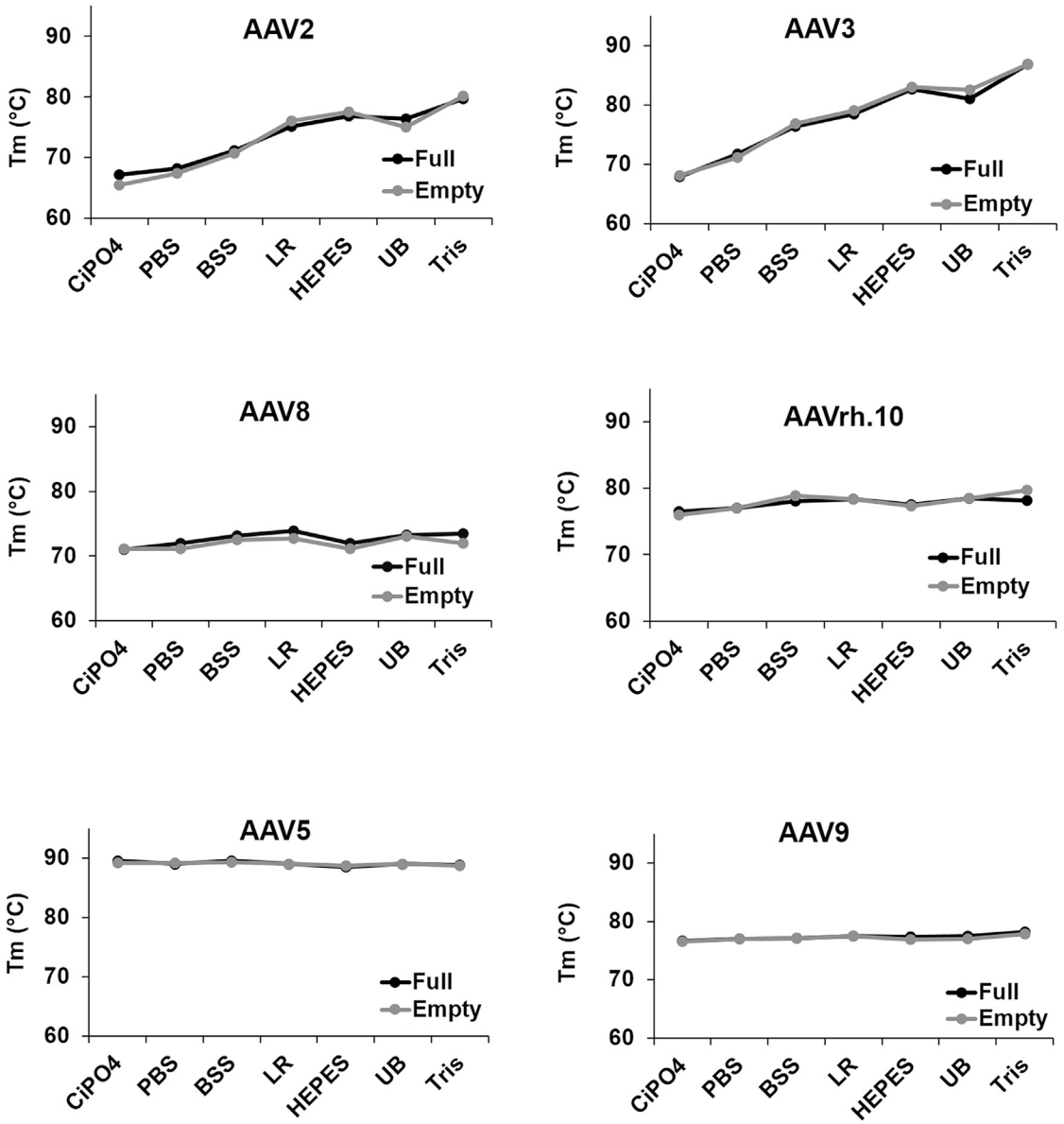

Figure 3. Comparative Analysis of the T_m of Full, Packaging GFP Transgene, and Empty Capsids in the Different AAV Formulation and Storage Buffers
Plots show T_m (°C) (y axis) versus buffer (x axis) for two selected rAAV serotypes from the buffer stability groupings. Group I was AAVs with T_ms varying by ~15°C–20°C, AAV2 and AAV3 (top); group II was AAVs with T_ms varying by ~3°C–6°C, AAV8 and AAVrh.10 (middle); and group III was AAVs with T_ms varying by <2.0°C, AAV5 and AAV9. The T_m of the full rAAV capsids is shown in a black line, and the empty capsids are shown in a gray line.

to identify AAV1, AAV2, AAV5, AAV6-K531E, AAV8, and AAV9.[38] Significantly, these previous studies used different biological "replicates" that were produced and purified using different protocols. The similarity of T_ms in the different buffers supports the validity of the DSF approach for serotype identification.

In addition to there being no significant difference between full and empty capsids (Figure 3; Table 1), the T_ms for full capsids packaging GFP or luciferase, e.g., AAV1 and AAV6, were the same in PBS (Figures 2A, 2F, and 5C). These data support the conclusion that the encapsulated genome is not a determinant of AAV capsid thermostability. It was recently reported, based on atomic force microscopy analysis of AAV2 empty capsids and those packaging single-stranded DNA (ssDNA) or self complementary DNA (scDNA) genomes, that the scDNA-containing capsid had greater resistance to deep deformation.[39] This information was revealed by quantitative statistical analysis because the observable correlations with genome content were minimal.[39] This observation implies that only a packaged

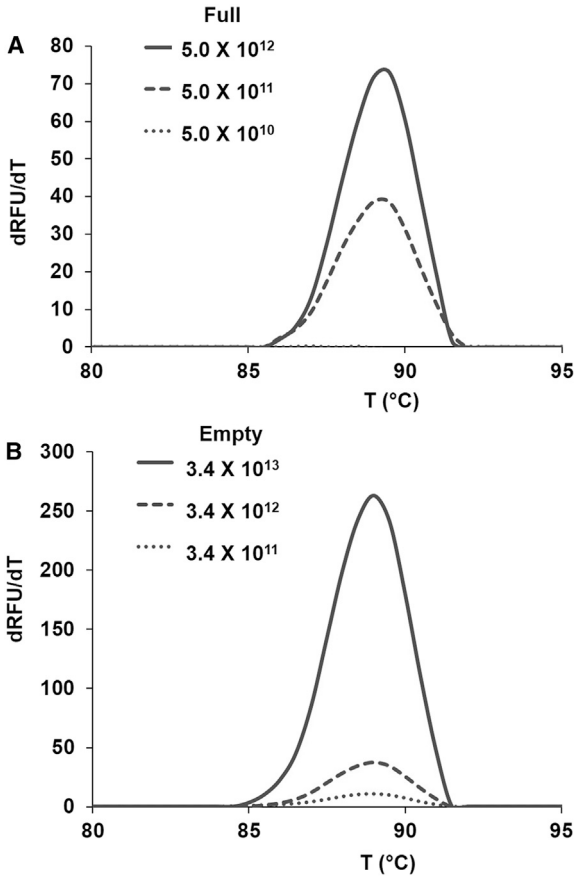

Figure 4. Concentration Survey of AAV5

(A) Full rAAV5-luc capsids at 5.0 × 10^{10}–5.0 × 10^{12} vg/mL. (B) Empty rAAV5 capsids at 3.4 × 10^{11}–3.4 × 10^{13} particles/mL. The inverted measured rate of change of fluorescence with time, dRFU/dT, is shown plotted in the y axis against T (°C) on the x axis.

double-stranded genome imparted mechanical AAV capsid stability, not ssDNA, compared to empty capsids, as reported here.

The observation that VP3 content alone is the determinant of AAV capsid stability ensures that vectors generated, with modified quantities of VP1 and VP2, can be analyzed by DSF (Figures 5A and 5B). The VP3 observation is consistent with previous reports, in which AAV5 containing a reduced VP1 content mixed with AAV2 with a higher VP1 content analyzed by DSF resulted in two distinct T_ms, corresponding to the T_m of AAV2 and AAV5 when tested alone.[35] These observations expand the utility of DSF for identification of WT AAV serotypes and chimeric or hybrid AAV vectors, which retain the complete VP3 sequence of one serotype. This is important because vectors with reduced VP1 content, often produced using the baculovirus/sf9, as for example, AAV5 and AAV8,[19,40,41] can be authenticated using DSF. This method is also thus applicable for vectors containing the VP1 of another serotype, e.g., the AAV2 VP1 incorporated into AAV5 and AAV8, to improve their infectivity.[41]

Previous analysis of the association energy and buried surface area for the symmetry-related VP:VP interactions of AAV1, AAV2, AAV5, and AAV8 capsids, based on the crystal structures, did not show any correlation with AAV capsid stability.[35,42] Data reported here indicate that AAV serotype stability is based on the amino acid sequence of VP3 and is governed by the ratio of basic:acidic residues, which is correlated to the pI of the capsids (Figure 6). The reversibility of the AAV1 and AAV6 T_ms by the single E531K difference (Figure 5C) confirmed this observation. The T_m for the AAV6-E531 variant is higher than that of AAV6 and equivalent to that of AAV1, whereas the T_m for the AAV1-K531 variant is equivalent to that of AAV6 within the ± 0.5°C error associated with these measurements. Thus, DSF has the ability to differentiate among AAVs that differ by a single amino acid, provided the amino acid difference causes a change in the overall charge and pI of the virus capsid.

The group I AAV serotypes, with highly variable T_ms in the different buffers, can have a broad tropism (e.g., AAV2)[1] or limited host tropism, for example, AAV3B.[43] The group II AAV serotypes, with intermediate variability in stability, can have limited tissue tropism, e.g., AAV1 for skeletal muscle[44] and AAV8, which targets the liver.[45] Finally, group III AAV serotypes, displaying little to no change in T_m in the different buffers, could also have broad (e.g., AAV9)[46,47] or limited tissue tropism (e.g., AAV5).[1] These observations show that storage buffer is not a determinant of tissue or cellular tropism, as was observed in the lack of any significant correlation with the level of gene expression in HEK293 cells (Figure 7). This suggests that the cellular or tissue environment encountered during infection dictates each AAV's transduction efficiency, consistent with observed differences in cell or tissue tropism during comparative infection analysis.[1,48]

In summary, DSF offers a rapid, cost effective, and robust method for AAV serotype identification in specific buffers because of their unique thermal stability profiles in the commonly utilized formulation and storage buffers. Table 1 reported here can serve as a "look up" reference table for the AAV serotypes tested because the data presented are reproducible, regardless of the source of sample production and method utilized for purification. The observation that capsid stability is based primarily on the charged VP3 residues ensures that T_m trends can be predicted for novel capsid variants compared to the WT virus. These data presented lead us to propose DSF as a method to be utilized for AAV vector identification post-storage and pre-administration as part of the quality control protocol for preclinical and clinical samples. Investigators should be able to add to the look up table for additional AAV serotypes or novel vectors of interest to expand it for all subsequent sample preparations.

MATERIALS AND METHODS

AAV Production

OneBac:*Sf9 rep/cap* producer cell lines of serotypes AAV1–AAV6, AAV8, AAV9, and AAVrh.10[19] were grown at 28°C in suspension culture under constant agitation to 1 L at 1.0 × 10^6 cells/mL and were infected with Bac-UF26-gfp at an MOI of 5.[19,49] The infected

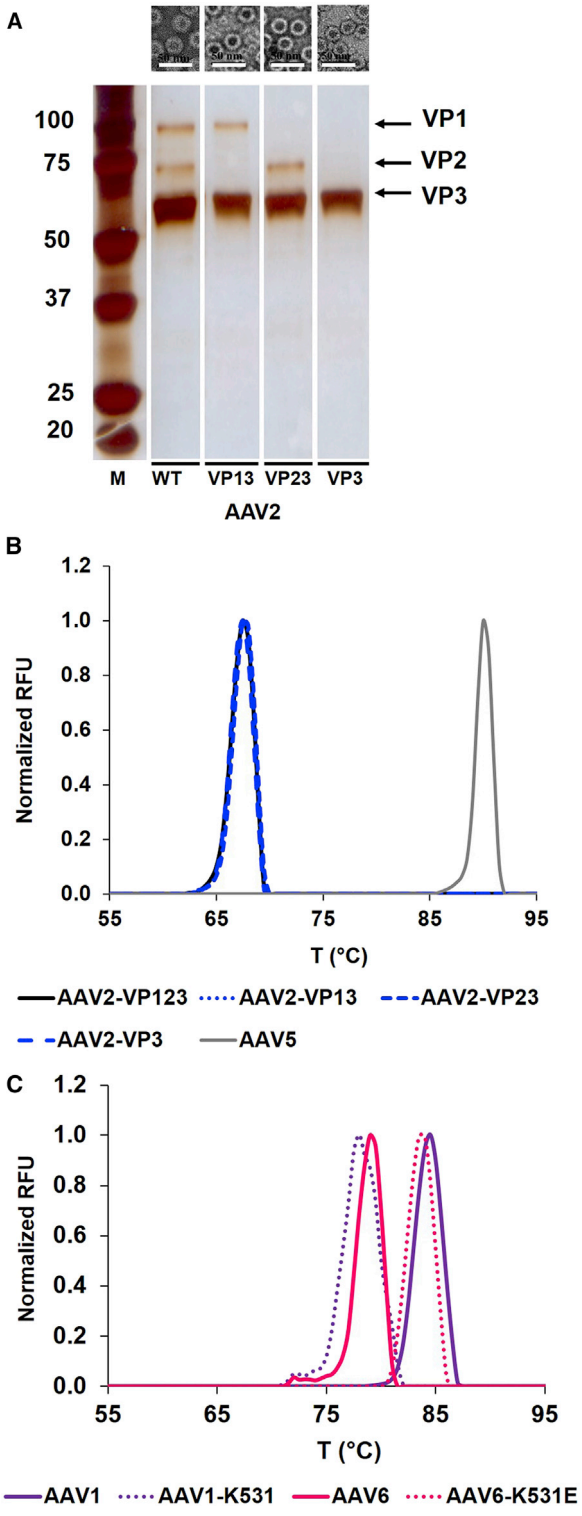

Figure 5. Sample Evaluation and Stability of WT and Mutant AAV2 VLPs

(A) Negative-stained EM (top) and silver-stained SDS-PAGE of AAV2-VP123 (WT), AAV2-VP13, AAV2-VP23, and AAV2-VP3 VLPs (bottom). Top: white scale bar, 50 nm. Bottom: the position of VP1, VP2, and VP3 is indicated with arrows. (B) Thermal profiles for AAV2-VP123 (WT), AAV2-VP13, AAV2-VP23, and AAV2-VP3 (different shades of blue), and rAAV5 (gray) VLPs. The AAV2 sample profiles are superposable and have identical T_ms of 67.5°C. (C) Thermal profiles (normalized RFU v T [°C] of full capsids of rAAV1-luc [purple], rAAV1-K531-luc [purple broken], rAAV6-luc [pink], and AAV1-E531-luc [pink broken]). The stabilizing/destabilizing effect of E531K is evident.

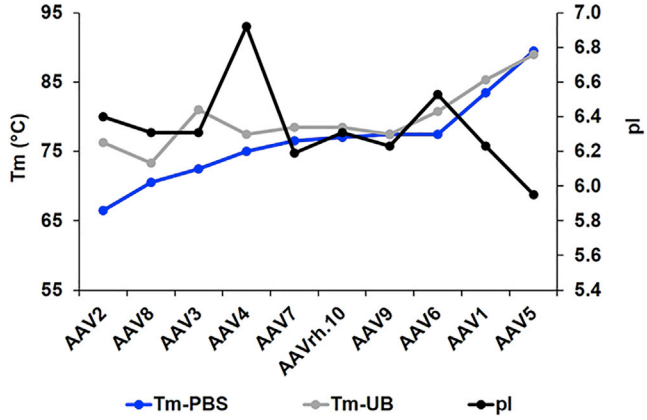

Figure 6. AAV Capsid T_m Is pI Dependent

A comparative analysis of the T_m of rAAV1–rAAV9 and AAVrh.10 in PBS and UB is plotted against the calculated capsid VP3 pI.

cells were harvested 72 hr post infection by centrifugation at 1.5K rpm in a JA-20 rotor. A successful infection was characterized by a bright green pellet due to intense GFP expression. The pellets were resuspended in TD buffer (1x PBS, 1 mM $MgCl_2$, and 2.5 mM KCl), and the supernatant was precipitated with 10% (w/v) PEG8000, as previously described.[50] The cell pellets were subjected to three freeze-thaw cycles in a dry ice/ethanol freezing bath and a 37°C water bath. After the third freeze-thaw cycle, the cell pellet and resuspended polyethylene glycol (PEG) pellet were treated with Benzonase (250 U) and incubated at 37°C for 30 min. Both solutions were clarified by centrifugation at 10,000 × *g* at 4°C for 20 min for purification (see below).

rAAV luciferase (rAAV1-luc, rAAV2-luc, rAAV5-luc, rAAV8-luc, rAAV7-luc, rAAV6-luc, rAAV6-E531-luc, and rAAV1-K531-luc) packaging vectors were produced by triple transfection in HEK293 cells. For this purpose, cells were seeded on 15-cm cell culture dishes. At a confluency of ~75%, the old growth medium was replaced with 15 mL of fresh DMEM. The three plasmids pHelper,[51] pTR-UF3-luc, and pXRAAV (for the respective virus as listed above) were mixed at an equimolar ratio (total: 40 µg to be used per 15-cm plate) and diluted in OptiMEM (Gibco) to a volume of 1 mL (per 15-cm plate). After adding 125 µL of polyethyleneimine (1 mg/mL), the solution was mixed, incubated at room temperature (RT) for 15 min, and added dropwise to the HEK293 cells. The following day, 5 mL of fresh DMEM were added to each plate. The cells were harvested after 72 hr and treated as described above for the *Sf9* cells.

The AAV2 VP variant VLPs were generated by site-directed mutagenesis (Agilent) of the AAV2 plasmid pFBDVPm11.[24] The VP1

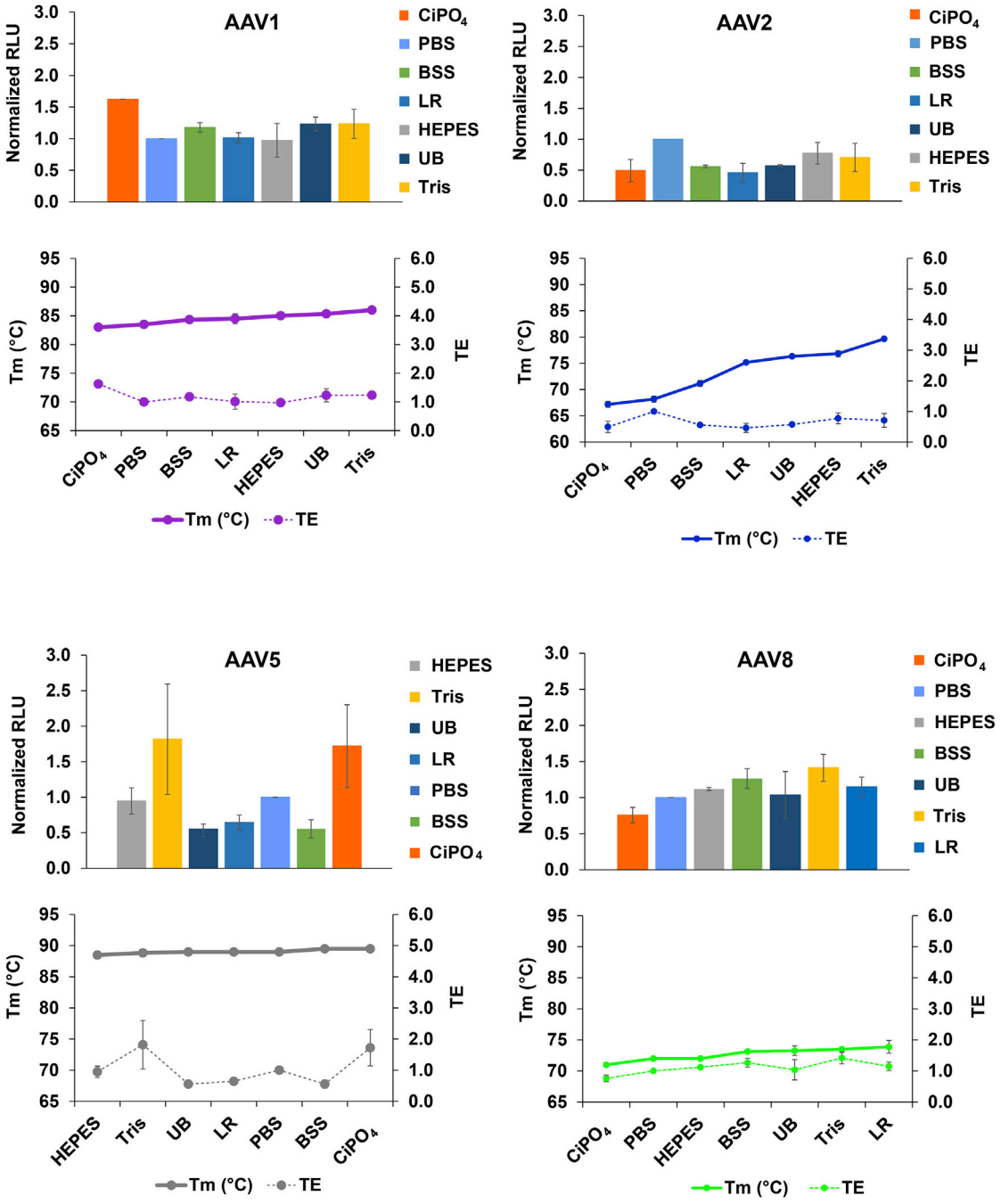

Figure 7. Transduction Efficiency of rAAV Diluted into Different Buffers

The normalized relative fluorescence (RFU) in HEK293 cells is shown for rAAV1-luc, rAAV2-luc, rAAV5-luc, and rAAV8-luc post incubation in the different buffers (as indicated on the right-hand side) above a plot of the T_m (left-hand side) and TE (right-hand side) against the same buffers. A similar trend in stability and TE is only observed for AAV8.

and VP2 start codons were mutated to GCG to generate AAV2-VP13, AAV2-VP23, and AAV2-VP3 only constructs. The WT and mutant plasmids were used to generate recombinant AAV2 VLPs in *Sf9* cells by the Bac-to-Bac expression system (Invitrogen) according to the manufacturer's protocol. The infected *Sf9* cells were harvested by centrifugation at 1,100 × *g* for 20 min in a JA10 rotor. The pellets were resuspended and prepared for purification as described above for the samples produced in the *Sf9* cell lines.

AAV Purification by AVB and Capture Select Affinity Ligand Column Chromatography Followed by Sucrose Gradient

The clarified supernatants from the various virus production protocols described above were diluted 1:1 with TD buffer and loaded onto a prepacked 1-mL AVB Sepharose HP column (GE Healthcare) (for AAV1–AAV8 and AAVrh.10) or a gravity flow column packaged from the capture select affinity ligand for AAV9 (CSAL9) at a flow rate of 0.5 mL/min. After loading, the column was washed with 20 mL of TD buffer. The virus was eluted with elution buffer (0.1 M NaAc and 0.75 M NaCl, pH 2.5), and the peak fractions were collected and neutralized with 1 M Tris-HCl, pH 10 (neutralization buffer), at a 1:10 ratio. The elution fractions that showed VP1, VP2, and VP3 on an SDS-PAGE gel were pooled, and the sample was concentrated to a volume of 500 μL and loaded onto a 5%–40% step sucrose gradient. Empty and full virus capsids were separated by centrifugation at 35K rpm in an SW41 rotor for 3 hr at 4°C. The empty capsids were extracted with a syringe from the 20%–25% sucrose fraction and the full capsids from the 30% to 35% fraction. The samples were buffer exchanged into 20 mM Tris-HCl, pH 7.4, and 150 mM NaCl and concentrated by pelleting at 50K rpm in an SW51 rotor. The pellet was resuspended in the Tris-HCl buffer, and the sample concentrations were determined by UV spectrometry for the empty capsids (E = 1.7 for concentration in mg/mL) and titers were determined by qPCR for full capsids, as previously described.[19]

Determination of the Thermal Stability of AAV Capsids by DSF

This method monitors the binding of the SYPRO Orange dye to hydrophobic regions of proteins that are exposed during unfolding. For the comparative analysis of full and empty capsids, 2.5 μL of each AAV serotype, at a concentration of 1×10^{14} vg/mL or 1 mg/mL (1×10^{14} particles), respectively, were added to 20 μL of each of the six commonly used buffer formulations for AAV vector storage and gene therapy applications and a newly developed buffer called UB (see formulation below). This buffer was created to overcome potential effects of temperature on pH when thermal stability assays are conducted at low pH and was included here as a control. The commonly used buffers include (1) PBS (10 mM Na_2HPO_4, 1.8 mM KH_2PO_4, pH 7.4, 27 mM KCl, and 137 mM NaCl), (2) citrate phosphate ($CiPO_4$) (0.2 M Na_2HPO_4 and 0.1 M citric acid, pH 7.4), (3) HEPES (50 mM HEPES, pH 7.4, 150 mM NaCl, and 2 mM $MgCl_2$), (4) Tris-HCl (Tris) (20 mM Tris-HCl, pH 7.4, 150 mM NaCl, and 2 mM MgCl), (5) Lactated Ringer (LR) (27.7 mM sodium lactate, pH 6.5, 102.7 mM NaCl, 4.0 mM KCl, and 1 mM $CaCl_2$), and (6) balanced salt solution (BSS) (109.5 mM NaCl, 10.1 mM KCl, 3.3 mM $CaCl_2$, 1.4 mM $MgCl_2$, 28 mM sodium acetate, and 5.8 mM sodium citrate, pH 7.4, with 0.02% Tween). The formulation for UB is 20 mM HEPES, 20 mM 2-(N-morpholino) ethanesulfonic acid (MES), 20 mM sodium acetate, pH 7.4, 150 mM NaCl, and 5 mM $CaCl_2$. In addition, 2.5 μL of 1% SYPRO Orange dye (Invitrogen) was added to each mixture to make a total reaction volume of 25 μL. The assays were run in a Bio-Rad MyiQ2 Thermocycler instrument, with temperature ranging from 30°C to 99°C and ramping at 0.5°C per step.[35] This protocol can be adapted for any qPCR instrument using filters commonly provided with the machines: FAM (485 nm) for excitation and ROX (625 nm) for emission. The rate of change of fluorescence with temperature was recorded, and the thermal profile is output as −dRFU/dT versus temperature. The thermal profile is then inverted by multiplying with −1 and normalized by dividing the raw values of the profile by the peak dRFU/dT value for evaluation. The peak value recorded on the thermogram is the T_m. A negative control 22.5 μL of each buffer and 2.5 μL of SYPRO Orange were included for each run. All experiments were conducted in triplicate each time using at least two biological replicates for all the samples tested, except for AAV4, which was repeated only twice with one biological sample due to a low sample yield.

To survey the minimal concentration of AAV capsid that would provide measurable fluorescence using DSF, AAV5, displaying the highest T_m, was used. AAV5 full and empty capsids, purified from a rAAV5-luc construct expressed in HEK293 cells, at 5×10^{13} vg/mL and 3.4×10^{14} particles/mL, respectively, were serially diluted 10–100x in PBS, and 22.5 μL of each dilution was used for the DSF analysis, as described above. To determine the role of the AAV VPs in capsid stability, WT AAV2 and VP variant VLPs were assayed, also in PBS, at a concentration of 1×10^{13} particles/mL, as described above, but without dilution because the samples were already in the assay buffer. To determine the role of basic and acidic residues in capsid stability, rAAV1-luc and rAAV6-luc and their variants, rAAV1-K531-luc and rAAV6-E531, at concentrations of $\sim 1 \times 10^{11}$–1×10^{12} vg/mL in PBS, were assayed by DSF, also as described above.

Transduction of HEK293 Cells by rAAV-luc Vectors in Different Buffer Formulations

The genome-containing titer of rAAV1-luc, rAAV2-luc, rAAV5-luc, and rAAV8-luc vectors, with a packaged luciferase transgene, were determined by qPCR, as previously described.[19] For the transduction assay, $\sim 2.5 \times 10^4$ HEK293 cells were seeded in a 96-well plate 1 day prior to infection. On the day of infection, the rAAV vectors were diluted into the six common AAV buffers plus UB (total volume: 10 μL) to infect cells at an MOI of 10^4 for AAV2 or 10^5 for AAV1, AAV5, and AAV8. The difference in the MOI used for AAV2 and the other AAVs stems from the higher transduction level observed for AAV2 in vitro compared to the other AAV serotypes tested.[1] The AAV-buffer mixtures were incubated at 4°C for 1 hr. Prior to infection, 90 μL of DMEM supplemented with 2% FBS and 1% antibiotic and antimycotic (ABAM) was added to the mixtures. The old media on the cells was discarded, and the virus-buffer-medium mixture (total volume: 100 μL) was added to the cells. After incubating the cells at 37°C and 5% CO_2 for 48 hr, the medium was removed and the cells were washed with PBS. For the luciferase assay, the cells were lysed and the luminescence was determined using the Luciferase Assay Kit (Promega), according to the manufacturer's protocol, on a Synergy HTX plate reader (BioTek).

AUTHOR CONTRIBUTIONS

A.B. and M.M. contributed to study conception, Figures 1–7, and manuscript preparation; S.P., A.J., and J.C.Y. contributed to Figures 1 and 2; B.L. and B.B. contributed to study conception; R.M. and

M.A.-M. are the grantees for this study and contributed to study conception and manuscript preparation.

CONFLICTS OF INTEREST

M.A.-M. is an SAB member for AGTC, StrideBio, Inc., and Voyager Therapeutics, Inc., is a consultant for Intima Biosciences, and has a sponsored research agreement with AGTC, Adverum Biotechnologies, and Voyager Therapeutics, Inc. These companies have interest in the development of AAV for gene delivery applications. M.A.-M. and M.M. are inventors of AAV patents licensed to various biopharmaceutical companies. M.A.-M. is a co-founder of StrideBio, Inc. This is a biopharmaceutical company with interest in developing AAV vectors for gene delivery application.

ACKNOWLEDGMENTS

We thank the University of Florida (UF) Interdisciplinary Center for Biotechnology Research (ICBR) electron microscopy laboratory for providing negative-stain EM services. We thank Joshua Hull for technical services. This work was supported by NIH grants R01 GM109524 and R01 GM082946 to R.M. and M.A.-M.

REFERENCES

1. Gao, G., Vandenberghe, L.H., Alvira, M.R., Lu, Y., Calcedo, R., Zhou, X., and Wilson, J.M. (2004). Clades of adeno-associated viruses are widely disseminated in human tissues. J. Virol. *78*, 6381–6388.
2. Rose, J.A., Maizel, J.V., Jr., Inman, J.K., and Shatkin, A.J. (1971). Structural proteins of adenovirus-associated viruses. J. Virol. *8*, 766–770.
3. Snijder, J., van de Waterbeemd, M., Damoc, E., Denisov, E., Grinfeld, D., Bennett, A., Agbandje-McKenna, M., Makarov, A., and Heck, A.J. (2014). Defining the stoichiometry and cargo load of viral and bacterial nanoparticles by Orbitrap mass spectrometry. J. Am. Chem. Soc. *136*, 7295–7299.
4. Girod, A., Wobus, C.E., Zádori, Z., Ried, M., Leike, K., Tijssen, P., Kleinschmidt, J.A., and Hallek, M. (2002). The VP1 capsid protein of adeno-associated virus type 2 is carrying a phospholipase A2 domain required for virus infectivity. J. Gen. Virol. *83*, 973–978.
5. Zádori, Z., Szelei, J., Lacoste, M.C., Li, Y., Gariépy, S., Raymond, P., Allaire, M., Nabi, I.R., and Tijssen, P. (2001). A viral phospholipase A2 is required for parvovirus infectivity. Dev. Cell *1*, 291–302.
6. Hastie, E., and Samulski, R.J. (2015). Adeno-associated virus at 50: a golden anniversary of discovery, research, and gene therapy success–a personal perspective. Hum. Gene Ther. *26*, 257–265.
7. Gray, J.T., and Zolotukhin, S. (2011). Design and construction of functional AAV vectors. Methods Mol. Biol. *807*, 25–46.
8. Flotte, T.R. (2005). Adeno-associated virus-based gene therapy for inherited disorders. Pediatr. Res. *58*, 1143–1147.
9. Srivastava, A. (2016). In vivo tissue-tropism of adeno-associated viral vectors. Curr. Opin. Virol. *21*, 75–80.
10. Chao, H., Liu, Y., Rabinowitz, J., Li, C., Samulski, R.J., and Walsh, C.E. (2000). Several log increase in therapeutic transgene delivery by distinct adeno-associated viral serotype vectors. Mol. Ther. *2*, 619–623.
11. Nathwani, A.C., Tuddenham, E.G., Rangarajan, S., Rosales, C., McIntosh, J., Linch, D.C., Chowdary, P., Riddell, A., Pie, A.J., Harrington, C., et al. (2011). Adenovirus-associated virus vector-mediated gene transfer in hemophilia B. N. Engl. J. Med. *365*, 2357–2365.
12. Gaudet, D., Méthot, J., and Kastelein, J. (2012). Gene therapy for lipoprotein lipase deficiency. Curr. Opin. Lipidol. *23*, 310–320.
13. Tardieu, M., Zérah, M., Husson, B., de Bournonville, S., Deiva, K., Adamsbaum, C., Vincent, F., Hocquemiller, M., Broissand, C., Furlan, V., et al. (2014). Intracerebral administration of adeno-associated viral vector serotype rh.10 carrying human SGSH and SUMF1 cDNAs in children with mucopolysaccharidosis type IIIA disease: results of a phase I/II trial. Hum. Gene Ther. *25*, 506–516.
14. Tseng, Y.S., Vliet, K.V., Rao, L., McKenna, R., Byrne, B.J., Asokan, A., and Agbandje-McKenna, M. (2016). Generation and characterization of anti-adeno-associated virus serotype 8 (AAV8) and anti-AAV9 monoclonal antibodies. J. Virol. Methods *236*, 105–110.
15. Tseng, Y.S., and Agbandje-McKenna, M. (2014). Mapping the AAV capsid host antibody response toward the development of second generation gene delivery vectors. Front. Immunol. *5*, 9.
16. Wobus, C.E., Hügle-Dörr, B., Girod, A., Petersen, G., Hallek, M., and Kleinschmidt, J.A. (2000). Monoclonal antibodies against the adeno-associated virus type 2 (AAV-2) capsid: epitope mapping and identification of capsid domains involved in AAV-2-cell interaction and neutralization of AAV-2 infection. J. Virol. *74*, 9281–9293.
17. Kuck, D., Kern, A., and Kleinschmidt, J.A. (2007). Development of AAV serotype-specific ELISAs using novel monoclonal antibodies. J. Virol. Methods *140*, 17–24.
18. Van Vliet, K., Mohiuddin, Y., McClung, S., Blouin, V., Rolling, F., Moullier, P., Agbandje-McKenna, M., and Snyder, R.O. (2009). Adeno-associated virus capsid serotype identification: analytical methods development and application. J. Virol. Methods *159*, 167–177.
19. Mietzsch, M., Grasse, S., Zurawski, C., Weger, S., Bennett, A., Agbandje-McKenna, M., Muzyczka, N., Zolotukhin, S., and Heilbronn, R. (2014). OneBac: platform for scalable and high-titer production of adeno-associated virus serotype 1-12 vectors for gene therapy. Hum. Gene Ther. *25*, 212–222.
20. Miller, E.B., Gurda-Whitaker, B., Govindasamy, L., McKenna, R., Zolotukhin, S., Muzyczka, N., and Agbandje-McKenna, M. (2006). Production, purification and preliminary X-ray crystallographic studies of adeno-associated virus serotype 1. Acta Crystallogr. Sect. F Struct. Biol. Cryst. Commun. *62*, 1271–1274.
21. Huang, X., Hartley, A.V., Yin, Y., Herskowitz, J.H., Lah, J.J., and Ressler, K.J. (2013). AAV2 production with optimized N/P ratio and PEI-mediated transfection results in low toxicity and high titer for in vitro and in vivo applications. J. Virol. Methods *193*, 270–277.
22. Rayaprolu, V., Kruse, S., Kant, R., Movahed, N., Brooke, D., and Bothner, B. (2014). Fluorometric estimation of viral thermal stability. Biol. Protoc. *4*, e1199.
23. Brooke, D., Mohaved, N., and Bothner, B. (2015). Universal buffers for use in biochemistry and biophysical experiments. AIMS Biophysics *2*, 336–342.
24. Urabe, M., Ding, C., and Kotin, R.M. (2002). Insect cells as a factory to produce adeno-associated virus type 2 vectors. Hum. Gene Ther. *13*, 1935–1943.
25. Warrington, K.H., Jr., Gorbatyuk, O.S., Harrison, J.K., Opie, S.R., Zolotukhin, S., and Muzyczka, N. (2004). Adeno-associated virus type 2 VP2 capsid protein is nonessential and can tolerate large peptide insertions at its N terminus. J. Virol. *78*, 6595–6609.
26. Rabinowitz, J.E., Xiao, W., and Samulski, R.J. (1999). Insertional mutagenesis of AAV2 capsid and the production of recombinant virus. Virology *265*, 274–285.
27. Sonntag, F., Schmidt, K., and Kleinschmidt, J.A. (2010). A viral assembly factor promotes AAV2 capsid formation in the nucleolus. Proc. Natl. Acad. Sci. USA *107*, 10220–10225.
28. Sievers, F., Wilm, A., Dineen, D., Gibson, T.J., Karplus, K., Li, W., Lopez, R., McWilliam, H., Remmert, M., Söding, J., et al. (2011). Fast, scalable generation of high-quality protein multiple sequence alignments using Clustal Omega. Mol. Syst. Biol. *7*, 539.
29. Gasteiger, E., Gattiker, A., Hoogland, C., Ivanyi, I., Appel, R.D., and Bairoch, A. (2003). ExPASy: the proteomics server for in-depth protein knowledge and analysis. Nucleic Acids Res. *31*, 3784–3788.
30. Wu, Z., Asokan, A., Grieger, J.C., Govindasamy, L., Agbandje-McKenna, M., and Samulski, R.J. (2006). Single amino acid changes can influence titer, heparin binding, and tissue tropism in different adeno-associated virus serotypes. J. Virol. *80*, 11393–11397.
31. Wright, J.F. (2008). Manufacturing and characterizing AAV-based vectors for use in clinical studies. Gene Ther. *15*, 840–848.
32. Aitken, M.L., Moss, R.B., Waltz, D.A., Dovey, M.E., Tonelli, M.R., McNamara, S.C., Gibson, R.L., Ramsey, B.W., Carter, B.J., and Reynolds, T.C. (2001). A phase I study

of aerosolized administration of tgAAVCF to cystic fibrosis subjects with mild lung disease. Hum. Gene Ther. *12*, 1907–1916.

33. Flotte, T.R., and Mueller, C. (2011). Gene therapy for alpha-1 antitrypsin deficiency. Hum. Mol. Genet. *20*, R87–R92.

34. Bainbridge, J.W., Smith, A.J., Barker, S.S., Robbie, S., Henderson, R., Balaggan, K., Viswanathan, A., Holder, G.E., Stockman, A., Tyler, N., et al. (2008). Effect of gene therapy on visual function in Leber's congenital amaurosis. N. Engl. J. Med. *358*, 2231–2239.

35. Rayaprolu, V., Kruse, S., Kant, R., Venkatakrishnan, B., Movahed, N., Brooke, D., Lins, B., Bennett, A., Potter, T., McKenna, R., et al. (2013). Comparative analysis of adeno-associated virus capsid stability and dynamics. J. Virol. *87*, 13150–13160.

36. Osting, S., Bennett, A., Power, S., Wackett, J., Hurley, S.A., Alexander, A.L., Agbandje-Mckena, M., and Burger, C. (2014). Differential effects of two MRI contrast agents on the integrity and distribution of rAAV2 and rAAV5 in the rat striatum. Mol. Ther. Methods Clin. Dev. *1*, 4.

37. Boye, S.L., Bennett, A., Scalabrino, M.L., McCullough, K.T., Van Vliet, K., Choudhury, S., Ruan, Q., Peterson, J., Agbandje-McKenna, M., and Boye, S.E. (2016). Impact of heparan sulfate binding on transduction of retina by recombinant adeno-associated virus vectors. J. Virol. *90*, 4215–4231.

38. Pacouret, S., Bouzelha, M., Shelke, R., Andres-Mateos, E., Xiao, R., Maurer, A., Mevel, M., Turunen, H., Barungi, T., Penaud-Budloo, M., et al. (2017). AAV-ID: a rapid and robust assay for batch-to-batch consistency evaluation of AAV preparations. Mol. Ther. *25*, 1375–1386.

39. Zeng, C., Moller-Tank, S., Asokan, A., and Dragnea, B. (2017). Probing the link among genomic cargo, contact mechanics, and nanoindentation in recombinant adeno-associated virus 2. J. Phys. Chem. B *121*, 1843–1853.

40. Mietzsch, M., Casteleyn, V., Weger, S., Zolotukhin, S., and Heilbronn, R. (2015). OneBac 2.0: Sf9 cell lines for production of AAV5 vectors with enhanced infectivity and minimal encapsidation of foreign DNA. Hum. Gene Ther. *26*, 688–697.

41. Kohlbrenner, E., Aslanidi, G., Nash, K., Shklyaev, S., Campbell-Thompson, M., Byrne, B.J., Snyder, R.O., Muzyczka, N., Warrington, K.H., Jr., and Zolotukhin, S. (2005). Successful production of pseudotyped rAAV vectors using a modified baculovirus expression system. Mol. Ther. *12*, 1217–1225.

42. Govindasamy, L., Padron, E., McKenna, R., Muzyczka, N., Kaludov, N., Chiorini, J.A., and Agbandje-McKenna, M. (2006). Structurally mapping the diverse phenotype of adeno-associated virus serotype 4. J. Virol. *80*, 11556–11570.

43. Ling, C., Lu, Y., Cheng, B., McGoogan, K.E., Gee, S.W., Ma, W., Li, B., Aslanidi, G.V., and Srivastava, A. (2011). High-efficiency transduction of liver cancer cells by recombinant adeno-associated virus serotype 3 vectors. J. Vis. Exp. 2538.

44. Elmallah, M.K., Falk, D.J., Nayak, S., Federico, R.A., Sandhu, M.S., Poirier, A., Byrne, B.J., and Fuller, D.D. (2014). Sustained correction of motoneuron histopathology following intramuscular delivery of AAV in pompe mice. Mol. Ther. *22*, 702–712.

45. Graham, T., McIntosh, J., Work, L.M., Nathwani, A., and Baker, A.H. (2008). Performance of AAV8 vectors expressing human factor IX from a hepatic-selective promoter following intravenous injection into rats. Genet. Vaccines Ther. *6*, 9.

46. Chen, B.D., He, C.H., Chen, X.C., Pan, S., Liu, F., Ma, X., Li, X.M., Gai, M.T., Tao, J., Ma, Y.T., et al. (2015). Targeting transgene to the heart and liver with AAV9 by different promoters. Clin. Exp. Pharmacol. Physiol. *42*, 1108–1117.

47. Dashkoff, J., Lerner, E.P., Truong, N., Klickstein, J.A., Fan, Z., Mu, D., Maguire, C.A., Hyman, B.T., and Hudry, E. (2016). Tailored transgene expression to specific cell types in the central nervous system after peripheral injection with AAV9. Mol. Ther. Methods Clin. Dev. *3*, 16081.

48. Zincarelli, C., Soltys, S., Rengo, G., and Rabinowitz, J.E. (2008). Analysis of AAV serotypes 1-9 mediated gene expression and tropism in mice after systemic injection. Mol. Ther. *16*, 1073–1080.

49. Aslanidi, G., Lamb, K., and Zolotukhin, S. (2009). An inducible system for highly efficient production of recombinant adeno-associated virus (rAAV) vectors in insect Sf9 cells. Proc. Natl. Acad. Sci. USA *106*, 5059–5064.

50. Zolotukhin, S., Potter, M., Zolotukhin, I., Sakai, Y., Loiler, S., Fraites, T.J., Jr., Chiodo, V.A., Phillipsberg, T., Muzyczka, N., Hauswirth, W.W., et al. (2002). Production and purification of serotype 1, 2, and 5 recombinant adeno-associated viral vectors. Methods *28*, 158–167.

51. Xiao, X., Li, J., and Samulski, R.J. (1998). Production of high-titer recombinant adeno-associated virus vectors in the absence of helper adenovirus. J. Virol. *72*, 2224–2232.